*Journal of the European Ceramic Society* **18** (1998) 229–235
© 1997 Elsevier Science Limited
Printed in Great Britain. All rights reserved
0955-2219/98/$19.00 + 0.00
PII: S0955-2219(97)00122-2

# Effects of Seeding on the Crystallisation Kinetics of Air-calcined Yttria-doped Hydrous Zirconia

J. Tartaj,* J. F. Fernández, C. Moure and P. Durán

Electroceramics Department, Instituto de Cerámica y Vidrio (CSIC), 28500-Arganda del Rey, Madrid, Spain

(Received 18 April 1997; accepted 16 June 1997)

## Abstract

*Yttria-doped tetragonal zirconia (Y–TZP, 3 mol% $Y_2O_3$) amorphous precursors seeded with nanometric Y–TZP particles (10 wt%) were prepared by the sol-precipitation method. Solid-state reactions occurring during heating were studied by differential thermal analysis and X-ray diffraction. It was found that the seeding of Y–TZP amorphous precursors with 10 wt% crystalline Y–TZP nanometric particles considerably lowered the onset of the Y–TZP solid solution crystallisation temperature by nucleation and epitaxial growth. Thus, a complete Y–TZP solid solution was formed in the temperature range of 320—350°C in air after a heat-treatment of 20 h, by seeding the Y–TZP amorphous precursors with 10 wt% of Y–TZP nanometric crystalline particles. The isothermal crystallisation kinetics for an unseeded and 10 wt% Y–TZP nanometric particles seeded Y–TZP precursors have been compared. The seeded Y–TZP precursors exhibited enhanced crystallisation kinetics (about one order of magnitude higher), and the activation energy for the Y–TZP solid solution crystallisation was reasonably lowered (from 184 kJ $mol^{-1}$ to 119 kJ $mol^{-1}$).* *© 1997 Elsevier Science Limited.*

## 1 Introduction

It is widely accepted that chemical methods of synthesis lead to powders with no compositional fluctuation and controlled particle shape and size.[1,2] However in most of them a metastable compounds are obtained needing a subsequent calcination step to convert the gels to oxide powder ceramics. In the last decade, the hydrothermal synthesis route, has been successfully used in many industrial processes for preparation of, for example, alumina in the Bayer process. This technique, although does not needs the calcination step to obtain oxides, but involves the use of relatively high temperatures (~300°C) and elevated pressures (> 100 MPa). Besides a further heat treatment at about 300°C becomes necessary to eliminate residual organic or inorganic products before using the ceramic powders. On the other hand, parameters like pH, concentration and liquid medium have to be carefully adjusted to obtain sinterable ceramic powders with controlled morphology. It is for these reasons that such a chemical route has not attracted the attention which has been paid to sol–gel or coprecipitation processing as the main routes to advanced ceramic powders.

In the case of the production of ultrafine yttria-doped tetragonal zirconia polycrystalline (Y–TZP) powders, a gel-precipitation technique using metal salts as chemical precursors has been widely used.[3–5] In such a chemical route, which involves the coprecipitation of metal hydroxides with ammonia, a thoroughly washing step with an alcohol play a crucial role to obtain dried powders with low strength agglomerates. The final step is the calcination of dried powders at temperatures ≈500°C leading to the crystalline Y–TZP powder with high intra-agglomerate porosity.[6,7] Such a heat treatment inevitably leads to the formation of strong interparticle bonds,[8] which detrimentally influence both the sinterability and the compaction capability of the so obtained Y–TZP powders. In order to get better powder characteristics the suggestion is to find the adequate processing which allows the use of Y–TZP crystallisation temperatures as low as to avoid the formation of the undesirable interparticle bonds.

---

*To whom correspondence should be addressed.

The claim of the present paper is the use, for the first time in the case of the Y–TZP, of the 'seeding fundamental concepts', successfully applied by the Messing[9–11] and Roy[12] groups in the case of the $Al_2O_3$ and the $Al_2O_3$–$SiO_2$ systems, to lowering the crystallisation temperature and/or modifying the crystallisation kinetics of the air-calcined Y–TZP precursors, as an alternative to other chemical routes.

## 2 Experimental procedure

The starting materials were co-precipitated gels. To do that $Zr(C_4H_9O)_4{\cdot}C_4H_9OH$ and $Y(NO_3)_3{\cdot}H_2O$ were dissolved in pure isopropanol slightly acidulated with $HNO_3$. This sol solution was labeled as A. On the other hand, a suspension of well crystallised Y–TZP seed particles (size ≅ 8 nm) in pure isopropanol was also prepared as described elsewhere.[4] The amount of seed particles was in proportion of 10 wt% relative to the final Y–TZP mass. This suspension was labeled as B. Then the sol solution A and the suspension B were mixed. To ensure a homogeneous dispersion of the Y–TZP seed particles, the sol solution containing the seeds was powerfully agitated for 1 h, and then coprecipitated with a mixture of pure isopropanol–$NH_4OH$ (1/1). The coprecipitate was filtered, washed with water to remove residual ammonium nitrate salt and, finally, thoroughly washed with pure isopropanol for five times and dried at 80°C in an oven. The dried powders were attrition milled for 2 h in pure isopropanol with zirconia ball and redried at 80°C overnight. The dried powders were heated in a small platinum crucible for soaking times which varied from 0·1 h up to 60 h in an isothermal mode in the temperature range of 320 to 400°C. After heating the amount of crystallised tetragonal phase was measured by X-ray diffraction (Siemens D5000 with $CuK_\alpha$) on the 111 peak area using a previously calibrated curve. A differential thermal analyzer (DTA/TG, Netzsch STA-409) was also used to study the onset, maximum and the end temperatures of the crystallisation process. The heating rate was in all cases of $5°C\,min^{-1}$. Specific surface area of the calcined Y–TZP powders was calculated by the BET-method (Accusorb 210E, Micromeritics), and the crystallite size $D_{111}$ of the powders was measured for the (111) reflection by X-ray line broadening using the Scherrer formula:[13] $D_{111}=0{\cdot}94\lambda/B_{111}\cos\theta$ where $B_{111}$ is the half width of the peak duly corrected for the effect of spectral and instrumental broadening. Powder morphology was observed by Scanning Electron Microscopy (SEM; Zeiss DSM 950) and Transmission Electron Microscopy (TEM; Jeol 2000FX).

## 3 Experimental results

### 3.1 Powder characteristics

Figure 1 shows the DTA thermograms for pure hydrous zirconia unseeded and 10 wt% seeded Y–TZP precursors. The effect of seeding in lowering the crystallisation temperature is clearly seen. The crystallisation temperature of Y–TZP in the maximum of the exothermic peak, from the 10 wt% seeded powder shifted ~35°C lower than that without seeding. In conjunction with the X-ray diffraction results in the heat treated samples, it was found that, as it is shown in Table 1, the temperature range in which the seeded Y–TZP crystallisation takes place is also larger (between ~305 and 560°C) than that of the unseeded sample (between ~370 and 560°C). Therefore the start of seeded Y–TZP crystallisation occurred at some 60°C lower than that of the unseeded sample. If, as suggested by Livage *et al.*[14] the crystallisation of pure tetragonal zirconia from amorphous phase started by nucleation at a favored points, then it should be assumed that an increasing of the nucleation density sites will shift the onset of the crystallisation to lower temperatures. In fact, as it is shown in Fig. 2, Y–TZP unseeded sample heat-treated for 40 h at 320°C remained almost amorphous, whereas a 10 wt% seeded Y–TZP sample was >80% crystallised at the same temperature for 20 h. Livage *et al.*[14] established that pure zirconia could start to crystallise at about 300°C and a minimum temperature of 350°C would be required for complete crystallisation. Theunissen *et al.*[15] observed the onset of crystallisation for Y–TZP solid solution at 400°C, and Boutz *et al.*[16] established by DSC experiments the amorphous to crystalline transition of Y–TZP at 450°C. According to our results both the decreasing in the onset of crystallisation temperature and the increasing of the Y–TZP

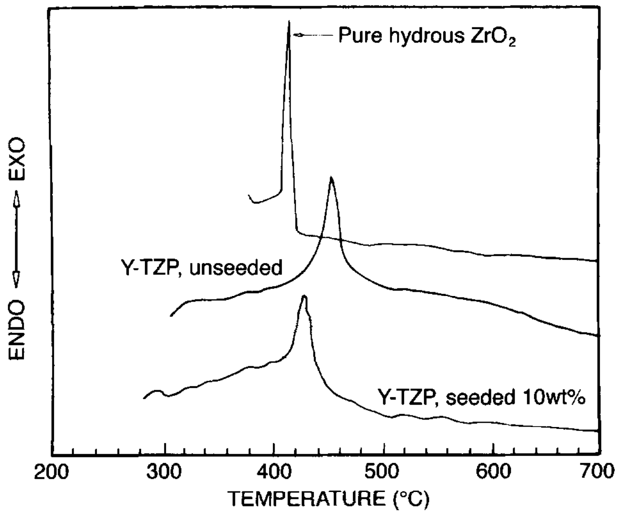

**Fig. 1.** DTA heating curves for pure hydrous zirconia, unseeded, and 10 wt% seeded Y–TZP amorphous precursors.

**Table 1.** DTA exothermic peak temperature (°C)

| *Samples* | *Onset* | *Maximum* | *End* |
|---|---|---|---|
| Unseeded Y–TZP | 365 | 455 | 560 |
| 10 wt% seeded Y–TZP | 305 | 425 | 560 |

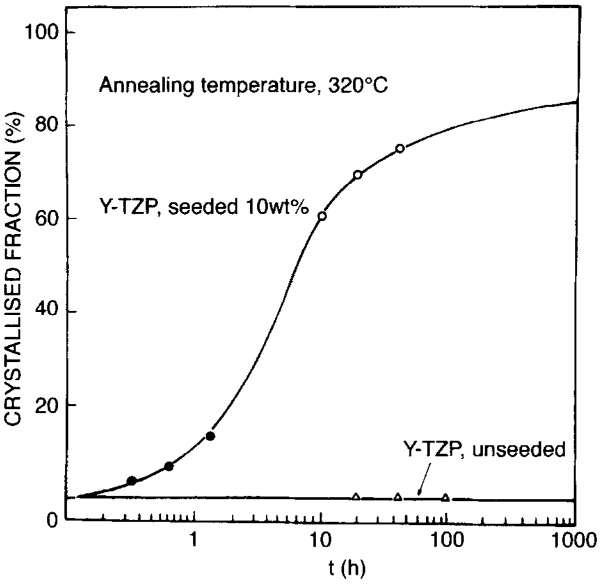

**Fig. 2.** XRD patterns for 10 wt% seeded and unseeded Y–TZP amorphous precursors heat-treated at 320°C for 20 and 40 h, respectively.

crystallisation rate could probably be attributed, in principle, to a lower activation energy required to nucleate the Y–TZP phase from the seeds.

After calcining the specific surface and the crystallite size of the unseeded and seeded powders were strongly influenced. As it is shown in Fig. 3, the unseeded powders were much more agglomerated than the seeded ones. The specific surface decreases as the calcination temperature increases, but such a decreasing is due to a higher crystallite size. The crystalline size (~15 nm) in the seeded powder was almost constant in the calcination temperature range which is consistent with an almost no variation of the specific surface (~100 $m^2 g^{-1}$) at those calcination temperatures. In the case of the unseeded powders the crystallite size increased, from ~11·3 nm at 350°C to ~14 nm at 400°C according to the crystallite growth of the newly-formed tetragonal zirconia solid solution. From the TEM studies, as it is shown in Fig. 4(b), well shaped tetragonal zirconia particles with sizes between 10 and 20 nm, were produced by air-calcining at 350°C for 30 h. Similar results were reported for tetragonal zirconia produced by hydrothermal treatment at 300°C for 24 h.[17] Figure 4(a) shows the poorly developed tetragonal zirconia particles from the unseeded air-calcined sample at the same experimental conditions.

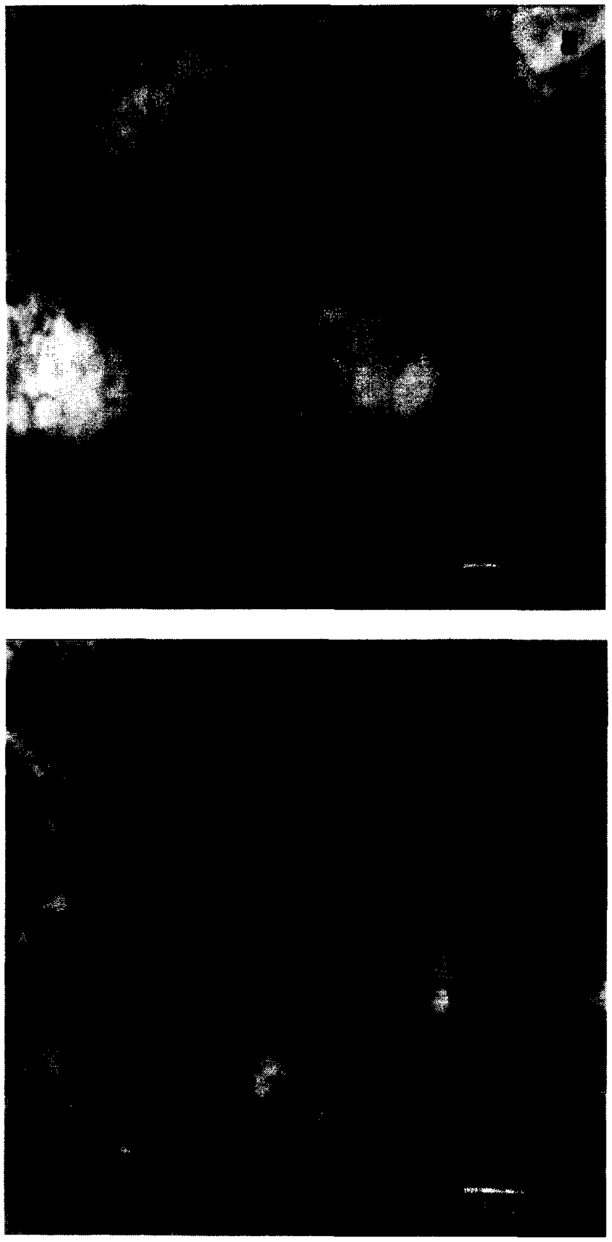

**Fig. 3.** SEM of (a) unseeded Y–TZP, and (b) 10 wt% seeded Y–TZP heat-treated at 350°C for 30 h.

Table 2 summarizes, as an example, the characteristics of two investigated powders, one of them, unseeded Y–TZP was calcined at 450°C for 5 h and the other one, Y–TZP seeded with 10 wt% nanocrystalline particles calcined at 375°C for 10 h. In both cases the porosity of the powders were mainly mesoporous but in the Y–TZP seeded sample a small amount of microporous was present ($S_{BET}-S_t$ = specific surface of microporous). Figure 5 shows the pore size distribution of unseeded Y–TZP(0) and the seeded Y–TZP(10) powders and, as it can be seen, the modal diameter of the unseeded Y–TZP powder (~8·4 nm) is higher than that of the seeded Y–TZP powder (6·4 nm). Taking into account these data and the crystallite size of both kinds of powders (8·4 and 15·4 nm, respectively), it could be stated that the pores are located between the crystallites and, therefore, the mesoporosity is

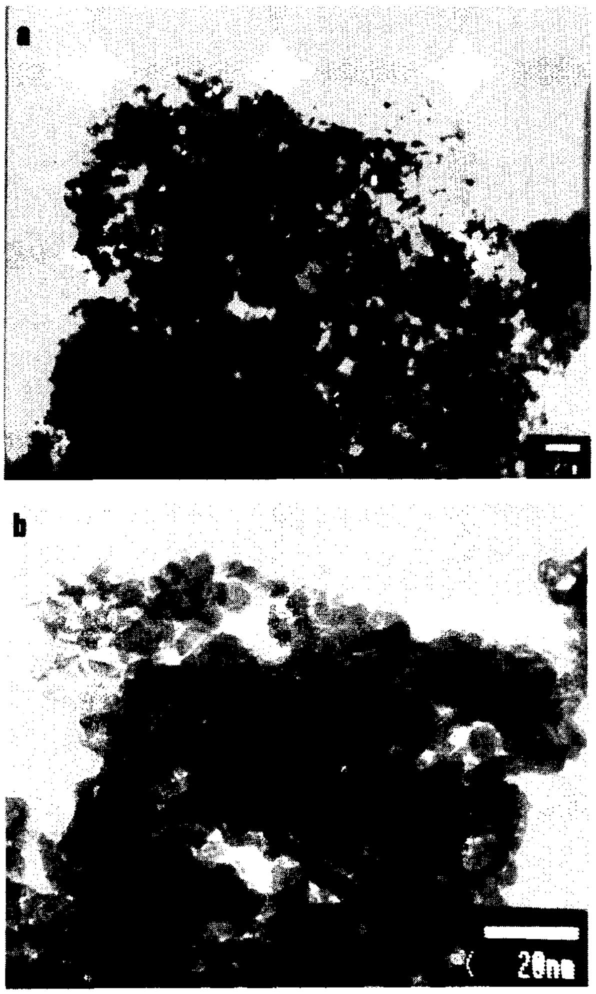

Fig. 4. TEM images of powders (a) unseeded Y–TZP and (b) 10 wt% seeded Y–TZP heat-treated at 350°C for 30 h.

Table 2. Main characteristics of unseeded Y–TZP(0) and 10 wt% seeded Y–TZP(10) powders calcined at 450°C 5 h and 375°C 10 h, respectively

| *Samples* | $S_{BET}$ $(m^2g^{-1})$ | $S_t$ $(m^2g^{-1})$ | $V_p$ $(cm^3g^{-1})$ | $P$ (%) | $R_p$ (nm) | $D_{XRLB}$ (nm) |
|---|---|---|---|---|---|---|
| Y–TZP(0) | 123 | 130 | 0·24 | 60 | 4·2 | 8·4 |
| Y–TZP(10) | 114 | 96 | 0·16 | 50 | 3·2 | 15·3 |

$S_{BET}$, BET surface area; $S_t$, specific surface of mesopores; $V_p$, mesopores volume; P, Intra-agglomerate porosity calculated as reported elsewhere;[16] $R_p$, the mode pore radii for maximum adsorption; $D_{RXLB}$, crystallite size as determined by X-ray line broadening.

mainly intra agglomerates. It is clear from the above data that well crystallized Y–TZP powders having specific surface areas $\geq 100\,m^2g^{-1}$ can be prepared by air calcining of the seeded Y–TZP amorphous precursors.

### 3.2 Crystallisation kinetics

If as it has been suggested[14,18] the crystallisation of tetragonal zirconia phase could be considered as a nucleation and growth process, then plotting the fraction of crystallised Y–TZP phase as a function of log time curves of the sigmoidal shape should be obtained in close agreement with the Avrami model,[19] which assumes that growth is controlled by nucleation. Figure 6 shows such a plot for unseeded and seeded Y–TZP precursors at 350°C. The curves have almost the same shape and slope which indicates that seeding does not influences the crystallisation mechanism but only the crystallisation rate. As it can be observed the influence of seeding on the crystallisation rate of Y–TZP is so high that the seeded crystallisation almost reaches completion as the unseeded crystallisation begins.

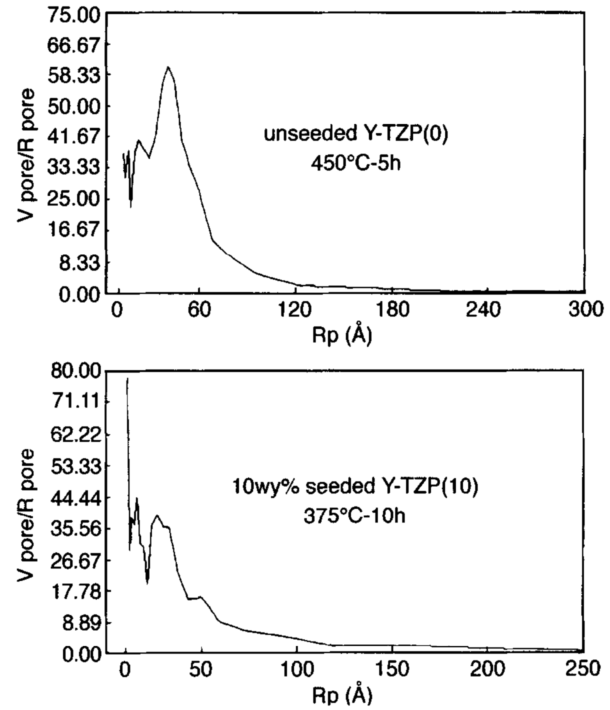

Fig. 5. Pore size distribution of unseeded Y–TZP(0) and 10 wt% seeded Y–TZP(10) powders at heat-treated at the indicated temperatures.

From the above results it seems evident that the kinetics of the Y–TZP crystallisation were reasonably enhanced by seeding Y–TZP amorphous precursors with polycrystalline Y–TZP nanometric particles. As established by the Avrami-type nucleation and growth kinetics,[19] an induction time in which no crystallisation was detected seems to exist. In our case, such an induction time was obtained by extrapolation of the linear part of the sigmoidal crystallisation curves to 0·5% of Y–TZP phase. Thus, as it can be observed, the induction time for the seeded Y–TZP crystallisation was reduced about one order of magnitude by comparison to the unseeded Y–TZP at the same temperature. On the other hand, the total time required for complete crystallisation of 10 wt% seeded Y–TZP was as short as 120 min at 400°C, whereas not less than 20 h were necessaries for complete crystallisation in the case of the unseeded Y–TZP.

According to the above assumption, the Avrami transformation kinetic expression[19] was used to

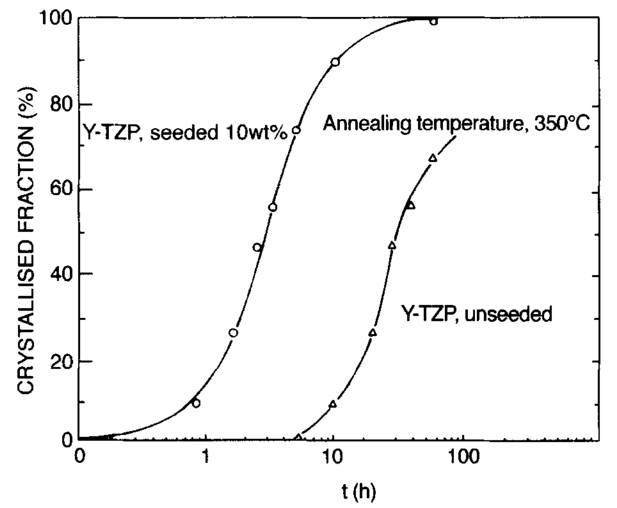

**Fig. 6.** Isothermal kinetics for the Y–TZP crystallisation at 350°C as a function of the Y–TZP seed concentration.

evaluate the XRD data. The relationship between volume fraction and time is given by

$$x = 1 - \exp(-kt^n) \qquad (1)$$

where n is a constant dependent on the nucleation and growth mechanisms, and k is the rate constant. For isothermal conditions, the experimental data were better fitted according to the following linear transformation of the above equation:

$$\ln[-\ln(1 - x)] = \ln k + n \ln t \qquad (2)$$

where x is the weight fraction of crystallised Y–TZP phase. Plots of ln[−ln (1−x)] as a function of ln t yields the values of n and k. The rate constants, shown in Table 3, were determined from the intercept at each isothermal temperature. As it is shown, comparable constants rate were measured at temperatures 50°C lower in seeded Y–TZP relative to unseeded samples.

The temperature dependence of k in eqn (1) apparently follows an Arrhenius relationship, according to:

$$k = A \exp(-E_a/RT) \qquad (3)$$

**Table 3.** Kinetic constant k, and activation energy, $E_a$, for the crystallisation of unseeded and 10 wt% seeded Y–TZP amorphous precursors

| *Temperature (K)* | *k (sec$^{-1}$)* | |
|---|---|---|
| | *Y-TZP (unseeded)* | *Y-TZP (seeded 10 wt%)* |
| 593 | — | $3{\cdot}20\times10^{-5}$ |
| 623 | $7{\cdot}21\times10^{-6}$ | $5{\cdot}75\times10^{-5}$ |
| 648 | $3{\cdot}20\times10^{-5}$ | — |
| 673 | $9{\cdot}98\times10^{-5}$ | $5{\cdot}88\times10^{-4}$ |
| $E_a$ (kJ mol$^{-1}$) | 184 ± 9·2 | 119 ± 6·0 |

where A is the frequency factor, $E_a$ the apparent activation energy of crystallisation, and R the gas constant. Plots of 1 g k versus 1/T, as shown in Fig. 7, yielded straight lines with very good correlation coefficients (0·99). The activation energies calculated were 184 ± 9·2 kJ mol$^{-1}$ and 119 ± 6 kJ mol$^{-1}$ for the unseeded and 10 wt% seeded Y–TZP amorphous precursors, respectively.

## 4 Discussion

The dehydration characteristics of zirconium gels and the pure zirconia crystallisation temperature (~430°C) are quite well established,[14,20–22] although the exothermicity produced as a consequence of the transition of the amorphous powder to crystalline tetragonal zirconia, termed as a glow phenomenon, has not been still clearly defined. As it was shown in Fig. 1, the incorporation of yttrium cations retarded the crystallisation of the amorphous hydrous zirconia powders from about 430°C up to 455°C. This result is in close agreement to those reported by other investigators, thus Mercera *et al.*[23] reported that the crystallisation of yttria-doped tetragonal zirconia occurred at 454°C, and the hydrous zirconia powders were still amorphous when calcined at 350°C for 15 h. Haberko *et al.*[24] reported a crystallisation temperature somewhat lower, ~437°C, for amorphous zirconia powder containing 3 mol% $Y_2O_3$. On that basis most of the research carried out on the study of Y–TZP sintering and properties currently used Y–TZP powders air calcined at temperatures higher than 500°C. At that calcination temperature the formation of

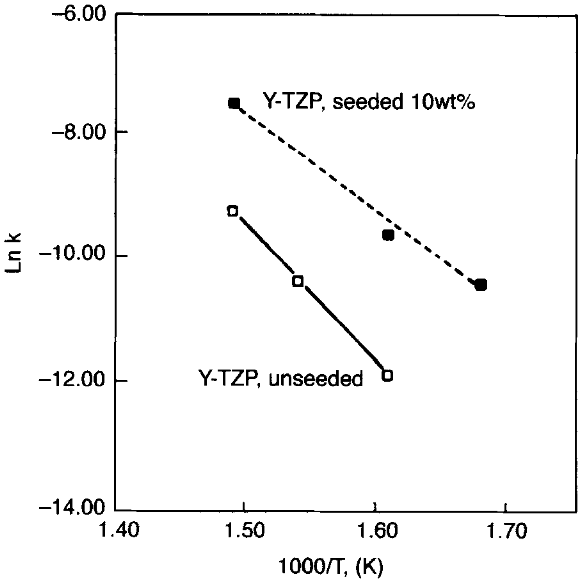

**Fig. 7.** Arrhenius plots of crystallisation rate constant for air-calcined unseeded and 10 wt% seeded Y–TZP amorphous precursors.

strong intercrystallite-bonds is favored which detrimentally influence the sinterability of the produced Y–TZP powders.[8,16]

The crystallisation of pure tetragonal zirconia, starting from amorphous $Zr(OH)_xO_y$ via hydrothermal synthesis, takes place by a topotactic crystallisation on the nuclei existing in the amorphous zirconia powders.[17] In the same way, it was reported the existence of an induction period previous to the tetragonal zirconia crystallisation confirming, thus, the idea of favored sites, as nuclei, for nucleation previously to the crystallisation.[14] This assumption, probably, would need to state a high activation energy to achieve a critical nuclei size. Table 1 and Fig. 6 showed that an increasing of the nucleation sites, by seeding, lowers the onset of the crystallisation of Y–TZP phase from the seeded powder at some 60°C lower than that without seeding. On the other hand, such an increasing of the nucleation sites results in an enhancing of the nucleation rate, see Fig. 6, and therefore giving rise to enhanced crystallisation kinetics for each temperature. These results are consistent with the fact that in the case of a heterogeneous nucleation process, as it can be considered the present case, the presence of the nanometric size Y–TZP seed particles requires a much smaller activation energy to reach the critical nuclei size.[25] Then we can conclude that the seeding of Y–TZP precursors with nanometric Y–TZP crystalline particles has a significant effect on the yttria-doped tetragonal zirconia crystallisation process, (a) by lowering the onset of the crystallisation temperature and (b) by enhancing the crystallisation kinetics at each temperature.

From the above results, it could be also stated that the characteristics of the seed Y–TZP nanometric particles, being isostructural with the final Y–TZP product and having a close lattice matching between them, will favour a decreasing of the activation energy for nucleation and reducing, thus, the overall energy requirements for epitaxial growth from the provided nuclei of the new synthesized Y–TZP phase.[24] Such a growth process could take place by a surface diffusion mechanism, which needs a low activation energy to be carried out. The stabilisation of tetragonal zirconia by the incorporation of $Y^{3+}$ cations as solid solution by the surface diffusion mechanism, on the other hand, results in a lowering of both the surface diffusion coefficient and the specific surface free energy of the zirconia.[23] As reported by Garvie [26] the surface free energy of tetragonal zirconia is lower than that of the monoclinic one.

The values obtained for the activation energy of crystallisation, in the case of Y–TZP amorphous precursors seeded with 10 wt% of nanometric Y–TZP crystalline particles, 119 ± 6 kJ $mol^{-1}$, is much smaller than those reported for the crystallisation of pure hydrous zirconia and doped-hydrous zirconia (4 mol% $Y_2O_3$), 232 and 262 kJ $mol^{-1}$, respectively.[27] These results supported the statement that the presence of nanometric Y–TZP seed particles lowered the activation energy to reach the critical nuclei size and, thus, the activation energy for the crystallisation process of the Y–TZP amorphous precursors.

The objective of the present work was not to study the effects of seeding on the morphology characteristics of the obtained powders, and its influence on the sintering behaviour of Y–TZP compacts. However, work is now in progress to elucidate it and the results will be reported soon in subsequent papers.

## 5 Conclusions

Summarising the above experimental results it could be concluded, on the basis of an assumed uniform distribution of zirconium and yttrium cations in an oxygen–hydroxyl–water matrix, as follows:

1. seeding with Y–TZP nanometric particles (10 wt%) induces a slight lowering (about 60°C lower) in the crystallisation temperature of the Y–TZP phase and a strong increase in the crystallisation rate (about one order of magnitude higher) of Y–TZP formed in air-calcined amorphous powders relative to the unseeded Y–TZP ones;
2. the mechanism for which such a process takes place is assumed to be a catalysed nucleation by the seeding of Y–TZP nanometric particles. The seeds being isostructural with the expected equilibrium phase and, therefore, having a close lattice matching, helps to control the thermodynamics of the reaction of formation of the Y–TZP solid solution. It seems be that a rapid inter-diffusion of the different ions takes place upon the seeds which acting as catalysts into the amorphous matrix controlling, thus, the growth process via, probably, epitaxial on the introduced nuclei;
3. the isothermal crystallisation process is best fitted by an Avramy-type kinetic relationship for a random nucleation which enhancing the crystallisation rate of Y–TZP, with an activation energies of 184 ± 9·2 kJ $mol^{-1}$ (44·16 ± 2·2 kcal $mol^{-1}$) and 119 ± 6 kJ $mol^{-1}$ (28·56 ± 1·44 kcal $mol^{-1}$) for unseeded and 10 wt% seeded Y–TZP amorphous powders, respectively. Since the Avrami model assumes

that growth is controlled by diffusion, then the low activation energy found for the Y–TZP crystallisation process support the contention of surface diffusion as the dominant mechanism for material transport at this thermal level.

## Acknowledgements

The authors express their appreciation to J. L. Baldonedo for assistance with the TEM and to the CICYT for financial support under the contract MAT-94-871.

## References

1. Aksay, I. A. Y., Shih, W., Sarikaya, M., Colloidal processing of ceramics with ultrafine particles. In *Ultrastructure Processing of Advanced Ceramics*, ed. J. D. Mackenzie and D. R. Ulrich, Wiley-Interscience, New York, 1988, pp. 393–407.
2. Brook, R. J., In *Concise Encyclopedia of Advanced Ceramic Materials*, ed. R. J. Brook. Pergamon Press, Oxford, 1991, pp. 1–8.
3. Haberko, K., Characteristics and sintering behaviour of zirconia ultrafine powders. *Ceramurgia Int.*, 1979, 5(4), 148–154.
4. Durán, P., Recio, P., Jurado, J. R., Pascual, C. and Moure, C., Preparation, sintering and properties of translucent $Er_2O_3$ doped tetragonal zirconia. *J. Am. Ceram. Soc.*, 1989, **72**, 2088–2093.
5. Groot Zevert, W. F. M., Theunissen, G. S. A. M., Winnubst, A. J. A. and Burgraaf, A. J., Powder preparation and compaction behaviour of ultra-fine Y–TZP. *J. Mat. Sci.*, 1990, **25**, 3449–3455.
6. Mercera, P. D. L., van Ommen, J. G., Dresbrug, E. B. M., Burggraaff, A. J. and Ross, J. R. H., Influence of ethanol washing of the hydrous precursor on the textural and structural properties of zirconia. *J. Mater. Sci.*, 1992, **27**, 4890–4898.
7. Durán, P., Villegas, M., Capel, F., Recio, P. and Moure, C., Low-temperature sintering and microstructural development of nanocrystalline Y–TZP powders. *J. Europ. Ceram. Soc.*, 1996, **16**, 945–952.
8. Readey, M. J., Lee, R., Holloran, J. W. and Heuer, A. H., Processing and sintering of ultrafine $MgO–ZrO_2$ and $(MgO–Y_2O_3)ZrO_2$ powders. *J. Am. Ceram. Soc.*, 1990, **73**, 1499–1503.
9. Kumagai, M. and Messing, G. L., Controlled transformation and sintering of a boehmite sol–gel by $\alpha$-alumina seeding. *J. Am. Ceram. Soc.*, 1985, **68**, 500–505.
10. Shelleman, R. S., Messing, G. L. and Kumagai, M., Alpha alumina transformation in seeded boehmite gels. *J. Non Cryst. Solids*, 1986, **82**, 277–285.
11. McCardlé, J. L. and Messing, G. L., Transformation and microstructure control in boehmite-derived alumina by ferric oxide seeding. *Adv. Ceram. Mater.*, 1988, **3**(4), 387–392.
12. Suwa, Y., Roy, R. and Komarneni, R., Lowering the sintering temperature and enhancing densification by epitaxy in structurally diphasic $Al_2O_3$ and $Al_2O_3$–MgO xerogels. *Mater. Sci. Engineer.*, 1986, **83**, 151–159.
13. Klug, K. P. and Alexander, L. E., *X-ray Diffraction Proceedures*, Chap. 9, Crystallite size and lattice strains from line broadening, John Wiley & Sons, New York, 1974, pp. 618–708.
14. Livage, J., Doi, K. and Mazieres, C., Nature and thermal evolution of amorphous hydrated zirconium dioxide. *J. Am. Ceram. Soc.*, 1968, **51**, 349–353.
15. Theunissen, G. S. A. M., Ph.D.thesis, University of Twente, Enschede, The Netherlands, 1991.
16. Boutz, M. M. R., Olde Scholtenhuis, R. J. M., Winnubst, A. J. A. and Burggraaff, A. J., A hydrothermal route for production of dense nanostructured Y–TZP. *Mat. Res. Bull.*, 1994, **29**, 31–40.
17. Tani, E., Yoshimura, M. and Somiya, S., Formation of ultrafine tetragonal $ZrO_2$ powders under hydrothermal conditions. *J. Am. Ceram. Soc.*, 1983, **66**(1), 11–14.
18. Denkewicz Jr, R. P., Tenhuisen, K. S. and Adair, J. H., Hydrothermal crystallisation kinetics of m-$ZrO_2$ and t-$ZrO_2$. *J. Mater. Res.*, 1990, **5**(5), 2698–2705.
19. Avrami, M., Kinetics of phase change. *J. Chem. Phys.*, 1939, **7** (12), 1103–1112; 1940, **8** (2), 212–224; 1941, **9** (2), 177–184.
20. Whitney, E. D., Observation on the nature of hydrous zirconia. *J. Am. Ceram. Soc.*, 1970, **53**, 697–698.
21. Torralvo, M. J., Alario, M. A. and Soria, J., The glow phenomenon in zirconium oxide. *J. Catal.*, 1964, **86**, 473–476.
22. Srinivasan, R., Harris, M. B., Simpson, S. F., de Angelis, R. J. and Davis, B. H., Zirconium oxide crystal phase. *J. Mater. Res.*, 1988, **3**(4), 787–797.
23. Mercera, P. D. L, van Ommen, J. G., Doesburg, E. B. M., Burggraaff, A. J. and Ross, J. R. H., Satabilized tetragonal zirconia as a support for catalyis. *Appl. Catal.*, 1991, **78**, 79–96.
24. Haberko, K., Ciesia, A. and Pron, A., Sintering behaviour of yttria-stabilized zirconia powders prepared from gels. *Ceramurgie, Int.*, 1975, **1**, 111–116.
25. Hulling, J. C. and Messing, G. L., Fundamental concepts for epitactic regulation of ceramic phase transformation. *Ceramic Trans.*, 1991, **22**, 401–414.
26. Garvie, R. C., Occurrence of metastable tetragonal zirconia as a cryustalline size effect. *J. Phys. Chem.*, 1965, **69**(4), 1238–1243.
27. Srinivasan, R., Muraleedharan, R. V., Roy, R. and Nayar, P. K. K., Dehydration and crystallisation kinetics of zirconia–yttria gels. *J. Am. Ceram. Soc.*, 1995, **78**(2), 429–432.